Introduction to "Handbook on Secondary Particle Production and Transport by High Energy Heavy Ions"

Takashi Nakamura,[1] **Lawrence Heilbronn**[2]
[1]Tohoku University, Cyclotron and Radioisotope Centre, Japan
[2]Lawrence Berkeley National Laboratory, University of California, USA

Abstract

With increasing the multi-purpose use of high energy, heavy ion accelerators, the secondary particle production and transport by high energy heavy ions are therefore current interesting topics. In this handbook, we have compiled the experimental results on DDX (double differential neutron production cross-section data), TTY (thick target neutron production yield data), heavy-ion produced neutron transport data, and spallation products production cross-section data taken at HIMAC. In addition to the HIMAC results, we have included some experimental results taken at other heavy ion accelerators of energies above about 100 MeV/nucleon. Also, we have included the calculation models and codes for heavy ion reaction and transport. The numerical data recorded in the CD-ROM is attached in the handbook. We do hope that this handbook will be useful for various applications.

1 Introduction

The high energy heavy ion accelerator facilitates the progress of accelerator science and research, such as the discovery of new super-heavy nuclei and unstable nuclei, clinical studies and treatments of the cancer therapy. The high energy heavy ion constituents of cosmic radiation must also be considered in space exploration. Heavy ion accelerator facilities are now operating or planned for construction in the world, and radioactive beam facilities using the spallation products from intense heavy ion beams are also under construction for these various purposes. In these high energy, heavy particle facilities many secondary particles are created from nucleus-nucleus interactions, and these particles, especially neutrons, can produce radioactivities induced in accelerator and structural materials, air, water, and soil, and can penetrate through the facility building into the surrounding environment. It is therefore quite necessary to evaluate the emission of secondary particles, especially neutrons and the creation of the residual nuclei in various materials, in order to estimate the source terms of accelerator shielding design, and also to calculate the dose delivered in the human body during the therapeutic irradiation.

When one of the editors, Takashi Nakamura, had performed the shielding design of the HIMAC facility (Heavy Ion Medical Accelerator in Chiba) at the National Institute of Radiological Sciences (NIRS), Japan more than 15 years before, there existed no available experimental data on neutron production from heavy ions and no available computer codes for the heavy-ion transport calculation at all. The HIMAC accelerator has being operated for heavy-ion therapy mainly using C ion beam and also opened for scientific research studies since 1994. A Japanese group (Tohoku University, High Energy Accelerator Research Organisation (KEK), Institute of Physical and Chemical Research (RIKEN), National Institute of Radiological Sciences (NIRS), headed by Takashi Nakamura) has done a series of systematic experiments on secondary particle production and transport by heavy ions over the past ten years from 1994. In 2000, an American group (Lawrence Berkeley National Laboratory (LBNL), Michigan State University, and Colorado University) co-ordinated by Lawrence H. Heilbronn, joined the HIMAC experiments.

We have compiled the experimental results on DDX (double differential neutron production cross-section data), TTY (thick target neutron production yield data), heavy-ion produced neutron transport data, and spallation products production cross-section data taken at HIMAC. In addition to the HIMAC results, we have included some experimental results taken at other heavy ion accelerators of energies above about 100 MeV/nucleon. Also, we have included the calculation models and codes for heavy ion reaction and transport. Our comprehensive experimental results are summarised in a handbook [1]. The handbook includes the following subjects: secondary neutron yields from thick targets, secondary neutron yields from thin targets, measurements of HZE neutrons behind shielding, production cross-sections of spallation products created in HZE reactions, moving source parameterisation of thick-target neutron yields and neutron production cross-sections, application of data to benchmark transport model calculations. The numerical data recorded in the CD-ROM is attached in the handbook. We do hope that this handbook will be useful for various applications, especially useful as benchmark data for Monte Carlo code analysis and evaluation.

2 Secondary neutron yields from thick targets

Table 1 lists the double differential (in energy and angle) thick-target (stopping length) neutron yield experiments summarised in a handbook [1]. The projectile and energy, target material and thickness, measured angle, and accelerator facility are shown. HIMAC is the Heavy Ion Medical Accelerator at the National Institute of Radiological Sciences in Chiba, Japan. NSCL is the National Superconducting Cyclotron Laboratory at Michigan State University in East Lansing, Michigan, USA. SREL is the now defunct Space Radiation Effects Laboratory that was located in Newport News, Virginia, USA. Bevelac is the now defunct high energy heavy ion accelerator that was at Lawrence Berkeley National Laboratory in Berkeley, CA, USA.

Table 1: Summarised lists of thick target neutron yield experiments using heavy ions [1]

Projectile (MeV/nucleon)	Targets (cm)	θ (deg)	Facility
He (100)	C (5.0) Al (4.0) Cu (1.5) Pb (1.5)	0 to 90	HIMAC
He (155)	Al (8.26)	10 to 160	NSCL
He (160)	Pb (3.9)	0 to 150	SREL
He (177.5)	C (14.7) H_2O (22.9) Steel (4.4) Pb (3.9)	0 to 150	SREL
He (180)	C (16.0) Al (12.0) Cu (4.5) Pb (5.0)	0 to 90	HIMAC
C (100)	C (2.0) Al (1.0) Cu (0.5) Pb (0.5)	0 to 90	HIMAC
C (155)	Al (8.26)	10 to 160	NSCL
C (180)	C (6.0) Al (4.0) Cu (1.5) Pb (1.5)	0 to 90	HIMAC
C (400)	C (20.0) Al (15.0) Cu (5.0) Pb (5.0)	0 to 90	HIMAC
Ne (100)	C (1.0) Al (1.0) Cu (0.5) Pb (0.5)	0 to 90	HIMAC
Ne (180)	C (4.0) Al (3.0) Cu (1.0) Pb (1.0)	0 to 90	HIMAC
Ne (400)	C (11.0) Al (9.0) Cu (3.0) Pb (3.0)	0 to 90	HIMAC
Si (800)	C (23.0) Cu (6.5)	0 to 90	HIMAC
Ar (400)	C (7.0) Al (5.5) Cu (2.0) Pb (2.0)	0 to 90	HIMAC
Fe (400)	C (6.0) Al (4.0) Cu (1.5) Pb (1.5)	0 to 90	HIMAC
Nb (272)	Nb (1.0) Al (1.27)	3 to 80	Bevalac
Nb (435)	Nb (0.51)	3 to 80	Bevalac
Xe (400)	C (3.0) Al (2.0) Cu (1.0) Pb (1.0)	0 to 90	HIMAC

As one example of these experimental results, Figure 1 gives the neutron energy spectra at angles of 0 to 90 degrees produced from thick C, Al, Cu and Pb targets bombarded by 400 MeV/nucleon C ions at HIMAC [2]. The neutron spectra were obtained by the TOF method using the NE213 scintillator. The measured spectra are compared with the PHITS (Particle and Heavy Ion Transport System) Monte Carlo code [3]. Three components can be clearly seen in the spectra. In general, the spectra in the forward direction have a broad peak at the high energy end. The peak energy usually occurs at about 60 to 70% of the beam energy per nucleon. As the target mass becomes lighter and the projectile mass increases, the high energy peak becomes more prominent. Most of the neutrons in this high energy, forward region come from the break-up of the projectile and direct knock-on processes. Neutrons with energies up to 2.5 times the incoming beam energy per nucleon can be produced by these processes. At energies below 20 MeV, the spectra are dominated by the breakup of the target. Because the target remnant is moving slowly in the lab frame, that source of neutrons is essentially isotropic. As such, target-like neutrons can be seen at all angles. As target mass increases, the relative contribution to the overall spectra from target breakup increases. At intermediate energies and intermediate angles, the spectra are dominated by the decay of the overlap region, where a sizeable number of projectile nucleons and target nucleons mix and can undergo several nucleon-nucleon collisions. The PHITS calculation gives good agreement with the measured spectra excluding the high energy region at 0 degree.

3 Secondary neutron yields from thin targets

Table 2 lists the double differential (in energy and angle) thin-target neutron yield (neutron production inclusive cross-section) experiments summarised in a handbook [1]. The projectile and energy, target material and thickness, measured angle and accelerator facility are shown in Table 2. RIKEN is the Institute of Physical and Chemical Research in Wako, Saitama, Japan.

Table 2: Summarised lists of thin target neutron yield experiments using heavy ions [1]

Projectile (MeV/nucleon)	Targets (g/cm^2)	Θ (deg)	Facility
He (135)	C(0.216), Al(0.162), Cu(0.268), Pb(0.340)	0 to 110	RIKEN
He (230)	Al(5.40), Cu(5.38)	5 to 80	HIMAC
C (135)	C(0.216), Al(0.162), Cu(0.268), Pb(0.340)	0 to 110	RIKEN
C (290)	C(1.80), Cu(4.47), Pb(2.27), marsbar(5.0)	5 to 80	HIMAC
C (400)	C(9.0), Cu(13.4), Pb(9.08)	5 to 80	HIMAC
N (400)	C(1.78), Cu(2.69)	5 to 80	HIMAC
Ne (135)	C(0.216), Al(0.162), Cu(0.268), Pb(0.340)	0 to 110	RIKEN
Ne (337)	C(3.06), Al(3.38), Cu3.81), U(5.60)	30 to 90	Bevalac
Ne (400)	C(1.80), Cu(4.47), Pb(2.27), ISS wall(2.97)	5 to 80	HIMAC
Ne (600)	Li(2.97), C(3.60), CH_2(2.40), Al(3.98), Cu(4.47), Pb(4.54), marsbar(5.0)	5 to 80	HIMAC
Ar (95)	C(0.216), Al(0.162), Cu(0.268), Pb(0.340)	0 to 110	RIKEN
Ar (400)	C(0.72), Cu(1.34), Pb(1.70)	5 to 80	HIMAC
Ar (560)	C(1.08), Cu(1.79), Pb(2.27), marsbar(5.0)	5 to 80	HIMAC
Fe (500)	Li(0.903), CH_2(0.957), Al(1.285)	5 to 80	HIMAC
Kr (400)	Li(0.47), C(0.55), CH_2(0.46), Al(0.54), Cu(0.90), Pb(1.02)	5 to 80	HIMAC
Xe (400)	Li(0.48), C(0.27), CH_2 0.2, 0.3), Al(0.26), Cu(0.45), Pb(0.57)	5 to 80	HIMAC

As one example of these experimental results, Figure 2 gives the neutron energy spectra at angles of 5 to 80 degrees produced from thick C, Cu and Pb targets bombarded by 290 MeV/nucleon C ions [4]. The neutron spectra were obtained by the TOF method using the NE213 scintillator. The measured spectra are compared with the moving source model [1], the QMD (Quantum Molecular Dynamics) code [5] and the HIC (Heavy Ion Collision) code [6]. At forward angles (0° for the RIKEN experiments, 5° for the HIMAC experiments), there is a prominent peak centred near the beam energy per nucleon. As the angle increases, the prominence of the peak decreases to a point at about 20° where the peak is insignificant. The high energy neutrons in the region of this forward peak come mainly from the breakup of the projectile, along with direct knock-out neutrons from the target. Neutrons are detected at energies 2 to 3 times the beam energy per nucleon, which is a phenomenon attributable to the collective Fermi motion inside the nucleus adding a momentum kick during the collision. At energies below 10-20 MeV, the spectra are dominated at all angles by the decay of the target remnant. The exponential behaviour of the cross-section with energy in this region suggests the target remnant decays by an equilibrium process. At intermediate energies (above 10 to 20 MeV, below the beam energy per nucleon), there is a component that becomes less pronounced as the angle increases. This component is dominated by the pre-equilibrium decay of the overlap region between the projectile and the target.

The moving source model consisting of three components above-described gives the best fit to the measured spectra, and the QMD code gives much better agreement with the measured ones than the HIC code based on the classical model of intranuclear-cascade reaction.

4 Measurements of HZE neutrons behind shielding

Recently, measurements have been made of neutrons behind shielding materials at heavy-ion accelerator facilities. Table 3 gives an overview of those experiments, showing the beams and targets used to produce the neutrons, the shielding material and thickness used, and the type of detection system used [1]. The experiments done with the 400 MeV/nucleon C beams were performed at HIMAC, and the 155 MeV/nucleon experiments were done at the NSCL. Another shielding experiment at HIMAC which is not included in Table 3 has been recently published [7].

Table 3: Summarised lists of neutron shielding experiments using heavy ion beams [1]

Projectile (AMeV)	Target used to produce neutrons	Shielding material	Range of shielding thicknesses	Detection system(s) used
C (400)	Cu	Concrete	0-250 cm	Self-TOF, NE-213, Activation foils
C (400)	Cu	Iron	0-100 cm	Self-TOF, NE-213
C (400)	Cu	Concrete Iron	0-400 cm 0-100 cm	TEPC
He, C, and O (155)	Hevimet	Concrete Iron	0-440 cm	Bonner Spheres

In HIMAC experimental arrangements, neutrons were produced by stopping 400 MeV/nucleon ^{12}C ions in a 5-cm thick Cu (10x10 cm square) target. The concrete and iron shields were 50- and 10-cm thick slabs, respectively, both of 100 × 100 cm square, and they were placed centered and normal to the beam axis. Figure 3 shows the neutron fluxes (# per steradian per MeV per ion) behind 0, 50, 100, 150, 200 cm of concrete, and 0, 20, 40, 60, 80, 100 cm of iron, using the self-TOF detector and the NE213 detector, together with the source neutron spectrum [8]. The self-TOF detector gives the neutron spectra above the low-energy threshold of 100 MeV because low energy recoils range out in the radiator, and below 600 MeV due to a lack of statistically-significant events. The spectra have a broad peak around 200 to 300 MeV, and little softening of the spectra can be seen with increasing shield thickness. The NE213 detector gives the neutron spectra from 20 to 800 MeV. Both spectra given by self-TOF and NE213 are generally in good agreement each other, although the broad peaks are not seen in the NE213 spectra. The dashed lines show MCNPX calculations of the spectra. The calculations, in general, give a harder spectrum than do the measurements. Below 100 MeV, the calculations overestimate the data as the shielding thickness increases. Between 100 and 400 MeV, the agreement between experiment and calculation is good. The agreement between calculation and experiment is quite good over the entire energy range (20-800 MeV) at 20 cm iron shield, and 50, 100, 150 cm concrete shields.

5 Production cross-sections of spallation products created in HZE reactions

An important component in the design of heavy-ion accelerator facilities is an accurate estimation of the radioactivities induced by spallation products in accelerator components and in shielding materials. To this end, the production cross-sections for various spallation products have been measured from heavy-ion reactions by several groups. Table 4 shows the various beams, targets and facilities used in the experiments [1]. PPA is the Princeton Particle Accelerator (now defunct) in USA and TWA-ITEP is the U10 synchrotron Terawatt Accumulator of the Moscow Institute for Theoretical and Experimental Physics in Russia.

The HIMAC series of experiments [9] used a target stack comprised of two to seven 5-mm thick Cu plates of 10 cm by 10 cm squares. In between each plate, samples of C (0.2-mm thick, 5 × 5 cm square), Al (0.1-mm thick, 9×10 cm^2), and Cu (0.1-mm thick, 9×10 cm^2) were placed in order to measure the spatial distributions of spallation products, and to determine the energy dependence on the cross-section. Foils of the same thickness were placed at the front of the stack to measure the reaction cross-sections and mass-yield distributions.

The data can be summed over the same mass numbers to produce mass-yield distributions. As one example, Figure 4 shows the mass-yield distributions (in mb) of 35 nuclides from ^{7}Be to ^{65}Zn for the 400-MeV/nucleon C and Ne ions interacting in a Cu target compared with the PHITS calculations. The PHITS calculations give good agreement with the experimental results, excluding an underestimation for some nuclides.

Table 4: Listing of the beams, energies (MeV/nucleon), targets and facilities used to measure spallation product cross-sections [1]

Beam	Energy	Target	Facility
^{14}N	278 AMeV	^{nat}Cu	PPA
^{12}C	2083 AMeV	^{nat}Cu	Bevalac
^{40}Ar	2000 AMeV	^{nat}Cu	Bevalac
^{12}C	2100 AMeV	^{nat}Cu	Bevalac
^{20}Ne	211 AMeV	^{nat}Cu	Bevalac
^{20}Ne	377 AMeV	^{nat}Cu	Bevalac
^{12}C	135 AMeV	^{nat}Cu	RIKEN
^{4}He	100 AMeV	C, Al, Cr, Fe, Ni, Cu, Pb	HIMAC
^{12}C	100 AMeV	C, Al, Cr, Fe, Ni, Cu, Pb	HIMAC
^{20}Ne	100 AMeV	C, Al, Cr, Fe, Ni, Cu, Pb	HIMAC
^{4}He	230 AMeV	C, Al, Cr, Fe, Ni, Cu, Pb	HIMAC
^{12}C	230 AMeV	Al, Cr, Fe, Ni, Cu, Pb	HIMAC
^{20}Ne	230 AMeV	C, Al, Cr, Fe, Ni, Cu, Pb	HIMAC
^{40}Ar	230 AMeV	C, Al, Cr, Fe, Ni, Cu, Pb	HIMAC
^{12}C	400 AMeV	C, Al, Cr, Fe, Ni, Cu, Pb	HIMAC
^{20}Ne	400 AMeV	C, Al, Cr, Fe, Ni, Cu, Pb	HIMAC
^{40}Ar	400 AMeV	C, Al, Cr, Fe, Ni, Cu, Pb	HIMAC
^{28}Si	800 AMeV	C, Al, Cr, Fe, Ni, Cu, Pb	HIMAC
^{12}C	200 AMeV	^{63}Cu, ^{65}Cu, Al, Co	TWA-ITEP

6 Conclusion

The work and data described here is from the efforts of scientists from Japan, the US, and Europe during the past 25 years. We have focused on research that is applicable to the general field of high energy (>100 MeV/nucleon), heavy ion transport. More specific applications in that field include accelerator design and shielding, medical physics and heavy-ion radiotherapy, and space-radiation transport and shielding design. It was our pleasure to survey the field to collect the most comprehensive data set we could find in four main areas: thick-target neutron yield measurements, neutron production cross-sections, measurements of neutrons behind shielding, and spallation products production cross-sections.

Acknowledgements

We, the editors, very gratefully acknowledge the following persons for giving us the numerical data together with the tables and graphs in their experimental and computational work:

For DDX (double differential neutron production cross-section data), Mr. Hisaki Sato, Tohoku University (Present address: Toshiba Co. Ltd.) and Dr. Yoshiyuki Iwata (NIRS). For TTY (thick target neutron production yield data), Dr. Tadahiro Kurosawa, Tohoku University (Present address: Advanced Institute of Science and Technology). For neutron transport data, Dr. Michiya Sasaki, Tohoku University (Present address: Central Research Institute of Electric Power Industries), Dr. Tomoya Nunomiya, Tohoku University (Present address: Fuji Electric Systems Co. Ltd.) and Dr. Reginald Ronnigen (Michigan State University). For spallation products production cross-section data, Dr. Hiroshi Yashima, Tohoku University (Present address: Research Reactor Institute, Kyoto University) and Dr. Yuri Titarenko (Institute for Theoretical and Experimental Physics, Russia). For moving source model, Dr. Takashi Kato, Tohoku University (Present address: Nikken Sekkei Co. Ltd.). For giving many references and supporting comments with the PHITS code, Dr. Hiroshi Iwase, Tohoku University (Present address: GSI (Gesellschaft fuer Schwerionenforschung), Germany).

References

[1] T. Nakamura, L. Heilbronn, *Handbook on Secondary Particle Production and Transport by High-energy Heavy Ions*, published by World Scientific in January 2006.

[2] T. Kurosawa, N. Nakao, T. Nakamura, H. Iwase, H. Sato, Y. Uwamino, A. Fukumura, *Phys. Rev.*, C 62 (2000) 044615.

[3] H. Iwase, K. Niita, T. Nakamura, *J. Nucl. Sci. Technol.* 39 (2002) 1142.

[4] Y. Iwata, T. Murakami, H. Sato, H. Iwase, T. Nakamura, T. Kurosawa, L. Heilbronn, R.M. Ronningen, K. Ieki, Y. Tozawa, K. Niita, *Phys. Rev.*, C 64 (2001) 054609.

[5] J. Aichelin, *Phys. Rep.*, 202 (1991) 233; K. Niita, S. Chiba, T. Maruyama, H. Takada, T. Fukahori, Y. Nakahara, A. Iwamoto, *Phys. Rev.*, C52 (1995) 2620.

[6] H.W. Bertini, T.A. Gabriel, R.T. Santoro, O.W. Hermann, N.M. Larson, J.M. Hunt, ORNL-TM-4134, Oak Ridge National Laboratory (1974).

[7] Y. Kumamoto, Y. Noda, Y. Sato, T. Kanai, T. Murakami, *Health Phys.*, 88 (2005) 469.

[8] M. Sasaki, E. Kim, T. Nunomiya, T. Nakamura, N. Nakao, T. Shibata, Y. Uwamino, S. Ito, A. Fukumura, *Nucl. Sci. Eng.*, 141 (2003) 140.

[9] H. Yashima, Y. Uwamino, H. Iwase, H. Sugita, T. Nakamura, S. Ito, A. Fukumura, *Radio Chimica Acta*, 91 (2003) 689: ibid. *Nucl. Instrum. Meth.*, B 226 (2004) 243.

Figure 1: Comparison of the measured neutron spectra with the PHITS calculations for 400 MeV/nucleon C ion on thick (stopping-length) C and Cu targets

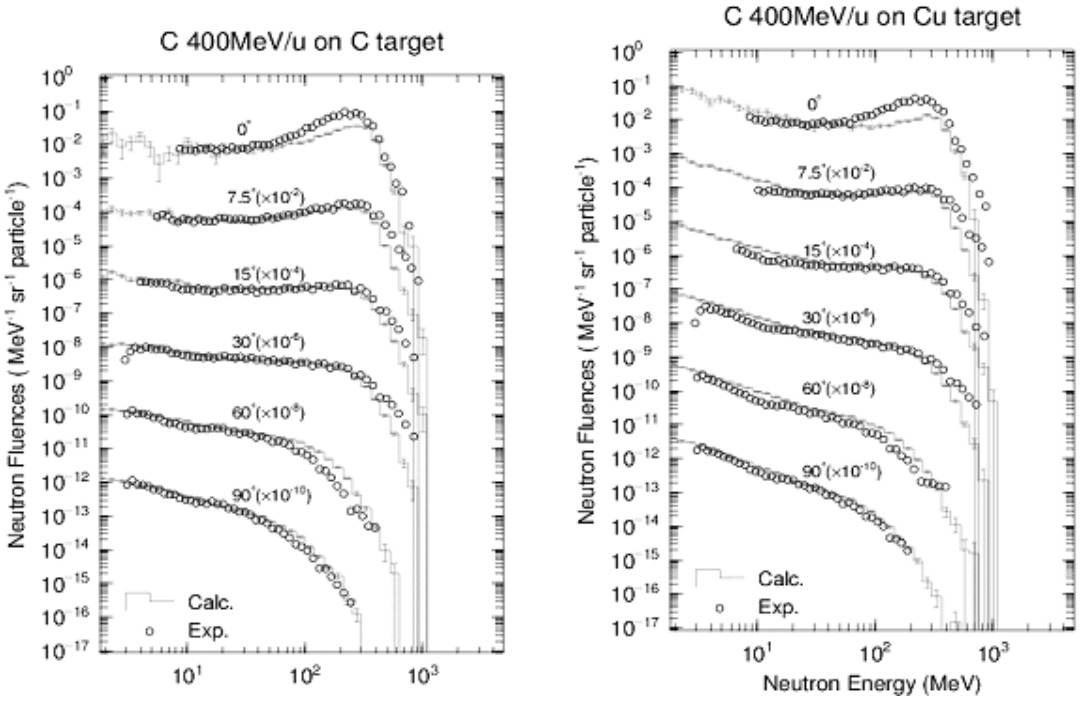

Figure 2: Double-differential neutron production cross-sections for 290 MeV/nucleon C ions

The targets are (a) C, (b) Cu and (c) Pb. The solid curves are the calculated results by the moving source model. The dashed and dot-dashed curves are the results of the QMD and HIC calculations, respectively.

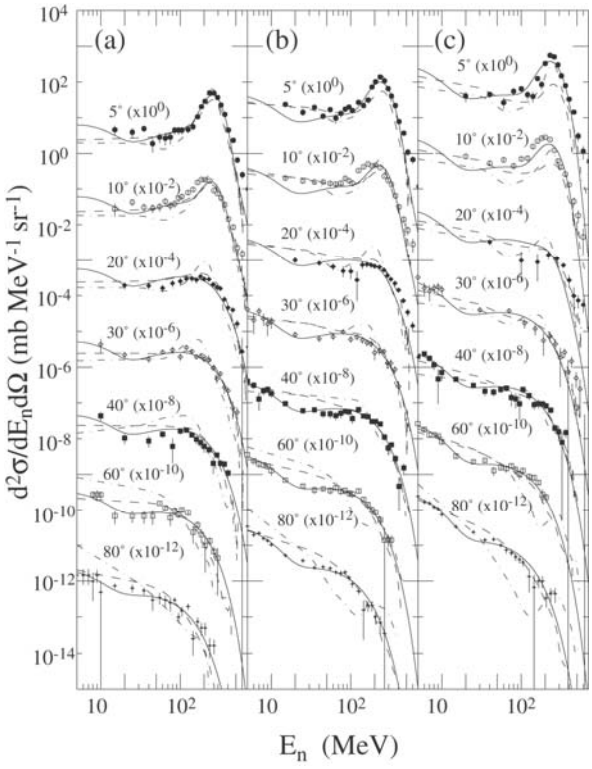

Figure 3: Comparison of measured and calculated neutron energy spectra penetrating through (a) concrete and (b) iron shields

Solid lines are the measured results of the self-TOF detector, dot-dash lines are of the NE213 detector. Dotted lines are the MCNPX calculations and broken line is the source neutron spectrum [2] generated from the Cu target bombarded by 400 MeV/nucleon C ions.

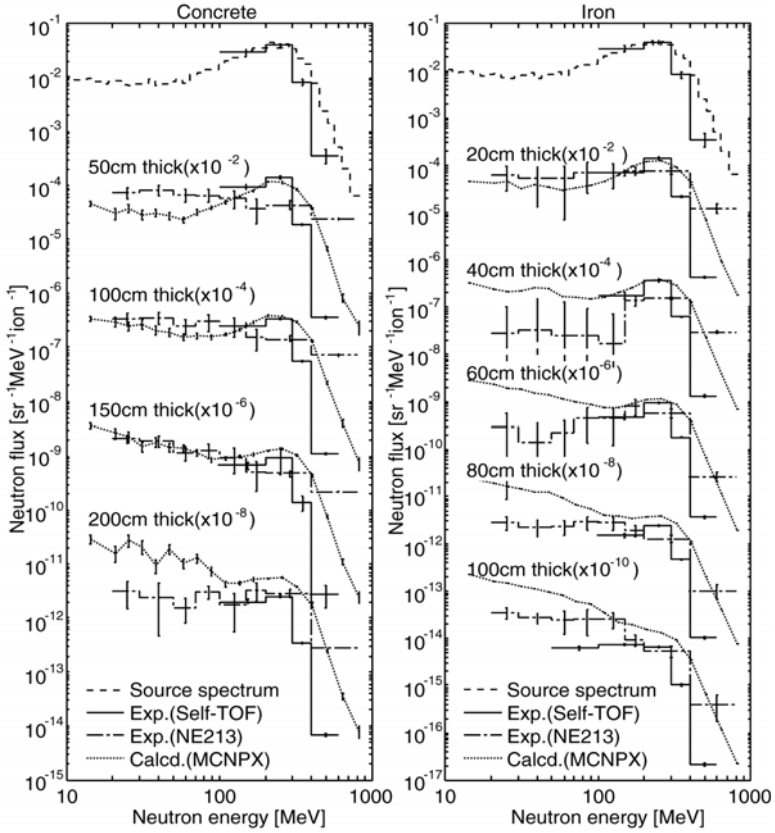

Figure 4: Comparison of measured and calculated reaction cross-sections of spallation products in Cu for 400 MeV/nucleon C and Ne projectiles with the PHITS calculations